MODELLING OF THE FORM OF ELECTRON BEAM WELDING JOINTS

Dipl. Mag. Tsonevska Tsvetomira[1], PhD student, Assoc. Prof. Dr. Eng. Koleva Elena[1], Eng. Asparuhova Boriana, PhD student, Assos. Prof. Dr. Olshanskaya Tatiana[2], Prof. DSc. Vutova Katia[1]

[1]Institute of Electronics, Bulgarian Academy of sciences, Bulgaria
[2]Perm National Research Polytechnic University, Perm, Russia

tsonevska@abv.bg, eligeorg@abv.bg, b_asparuhova@abv.bg

Abstract: *This article discusses a modelling approach for the welded seam form obtained by electron beam welding based on experimental data and types of mathematical functions. The process of electron beam welding is carried out by dividing the electron beam into two parts, resulting in the formation of two liquid baths. The samples that are welded are made of stainless steel with a change in process parameters: the distance between the two electron beam parts and the ratio of the power distribution between the two beam parts, the frequency of the deflection signal, the beam current, and the welding speed. Focusing current is of constant value. The weld cross sections shown in different process parameters are used to evaluate their shape using standard mathematical function - Gaussian functions.*

Keywords: electron beam welding; geometrical characteristics of the welds, stainless steel, statistical modelling, Gaussian functions.

1. Introduction

Electron Beam Welding (EBW) is a highly efficient and precise welding method, which is increasingly used in manufacturing and is of growing importance in different industrial areas such as the automobile and aerospace sectors. Electron Beam Welding (EBW) is a fusion welding process, during which intensive electron beams are implemented for processing of the materials being joined. The work-pieces melt as the kinetic energy of the electrons is transformed into heat during the interaction with the welded materials. EBW is the most widely applied method among the special welding methods. The reason for this is the possibility of obtaining very deep and narrow welds with good physical and mechanical properties with minimal structural changes and thermal deformations of the welded parts. Most of the advantages of EBW are based on the use of the high power density of the electron beam and the possibility to control it easily. Vacuum as working environment and the big working distance of the electron gun to treated sample surface are also positive features of the process. It is possible to process at high welding speeds, the need for subsequent mechanical and thermal treatment in a number of cases is eliminated, welding is possible near thermally unstable structural elements, the cost of materials (no special welding electrodes are needed) is reduced and the use of materials is improved [1].

Many analytical heat transfer models based on different 2-D or 3-D of the electron beam thermal source models have been developed [2, 3]. Solutions of these models give the shape and the dimensions of the weld pool. There are many EBW process parameters that influence the temperature field formation like: the input energy distribution, the welding speed, material properties, beam focus position, sample surface distance, emittance and brightness of the beam etc.

In this article, parameter dependent Gaussian model is proposed for fitting welded shapes $F(\vec{p})$, given by the equation:

$$F(\vec{p})=a_1(\vec{p})e^{\left[-\left(\frac{y-b_1(\vec{p})}{c_1(\vec{p})}\right)^2\right]}+a_2(\vec{p})e^{\left[-\left(\frac{x-b_2(\vec{p})}{c_2(\vec{p})}\right)^2\right]}+a_3(\vec{p})e^{\left[-\left(\frac{x-b_3(\vec{p})}{c_3(\vec{p})}\right)^2\right]} \quad (1)$$

where a is the amplitude, b is the centroid (location), c is related to the peak width, $\vec{p}$ is the vector of process parameter values (in coded units, Table 1), x is the coordinate in the cross-section, perpendicular to the beam movement direction.

The comparison between the estimated mathematical functions is performed on the base of the calculated confidence bounds for the fitted coefficients. The confidence bounds for fitted coefficients are given by:

$$C=b\pm t\sqrt{S} \quad (2)$$

where b are the coefficients produced by the fit, t is the inverse of Student's T cumulative distribution function, and S is a vector of the diagonal elements from the covariance matrix of the coefficient estimates, $(X^TX)^{-1}s^2$, X is the design matrix, X^T is the transpose of X, and s^2 is the mean squared error [4].

2. Experimental conditions

During this investigation 19 experiments of EBW of stainless steel samples is considered. The formation of a specific penetration zone configuration in the transverse weld joint section with an enlarged upper part and a narrow part of the joint weld is observed during the experiments (Fig. 1).

Fig. 1 *Weld cross-section, obtained at: L= 6 mm, F = 3 kHz, γ = 0, v = 5 mm/s, I_b = 55 mA.*

The electron beam welding process was held with beam deflection into two parts thus performing dual-pool welding. Weld seam quality is the main advantage of multi-pool welding, at which more homogenous weld seams are produced. Porosity and the root spiking are considerably reduced. The deflection was performed by transmitting rectangular signal to the deflection coils.

Table 1: *Regions of variation of the EBW process parameters.*

Factor (Z_i)	Dimension	Coded	Lower level (Zimin)	Upper level (Zimax)
L - Z_1	mm	p_1	2	6
F - Z_2	kHz	p_2	3	20
γ - Z_3	-	p_3	-0.3	0.3
v - Z_4	mm/s	p_4	5	15
I_b - Z_5	mA	p_5	40	64.5

Several process parameters have been varied during the experiments in order to investigate their influence on the shape of the welded seams (Table 1). Parameter L is the distance between the two beams (pools) (Z_1, mm), F is the frequency of the deflection signal (Z_2, kHz).

The energy distribution between the two resulting beams (Z_3) is determined by the parameter γ (gamma):

$$\gamma = (P_2-P_1)/(P_1+P_2), \qquad (3)$$

where P_1 and P_2 are the corresponding beam powers – on the front and on the back beams. If γ has a positive value then the back electron beam has more power than the front one. The welding speed is v (Z_4, mm/s) and I_b and I_f are the beam current (Z_5, mA) and the focusing current I_f. The focusing current was kept constant I_f = 835 mA. The EBW parameter variation regions for this experiment are presented in Table 1.

3. Gaussian and regression models for the shape of the welds

For each obtained experimentally weld cross-section shape individual model, representing a sum of three Gaussian terms (individual Gaussian function) is fitted:

$$F_i = a_{1i} e^{\left[-\left(\frac{y-b_{1i}}{c_{1i}}\right)^2\right]} + a_{2i} e^{\left[-\left(\frac{x-b_{2i}}{c_{2i}}\right)^2\right]} + a_{3i} e^{\left[-\left(\frac{x-b_{3i}}{c_{3i}}\right)^2\right]} \qquad (4)$$

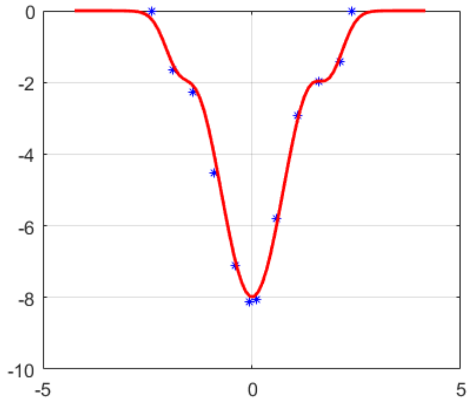

***Fig. 2** Weld cross-section: * - experimental, 'line' - calculated, weld width B=4.8 mm, weld depth H = 8.13 mm (L= 6 mm, F = 3 kHz, γ = 0, v = 5 mm/s, I_b = 55 mA)*

For example, for the presented in Fig. 1 weld the following individual Gaussian model is estimated:

$$F = -1.188573 e^{\left[-\left(\frac{y+1.776740}{0.448742}\right)^2\right]} - 7.988960 e^{\left[-\left(\frac{x-0.008903}{1.090250}\right)^2\right]} - 1.427782 e^{\left[-\left(\frac{x-1.872780}{0.466039}\right)^2\right]} \qquad (5)$$

In Fig. 2 is presented the calculated weld cross-section shape with weld width B=4.8 mm, weld depth H = 8.13 mm, obtained at process parameter values L= 6 mm, F = 3 kHz, γ = 0, v = 5 mm/s, I_b = 55 mA. The experimental weld dimensions are presented with '*'. It can be seen that the predicted shape of the weld coincides very well with the experimental one.

For all 19 experiments the values of the estimated coefficients a_1, b_1, c_1, a_2, b_2, c_2, a_3, b_3, c_3 are given in Table 2, together with the determination coefficients (R^2) and the adjusted determination coefficients (R_{adj}^2) in percent, which are measures for the accuracy of the estimated models (the closer 100% the better the model is).

***Table 2:** Coefficients from individual Gaussian models.*

N	a_1	b_1	c_1	a_2	b_2	c_2	a_3	b_3	c_3	R^2, %	R^2_{adj}, %
1	-1,508943	-1,570450	0,474859	-5,917234	-0,022202	1,221080	-0,699475	1,833090	0,351330	99.65	99.61
2	-0,875037	-1,735090	0,377790	-7,647232	0,025304	1,266160	-1,410696	1,677270	0,453985	99.76	99.73
3	-1,804751	-1,922270	0,527730	-7,868287	-0,010511	1,249500	-1,994837	2,015370	0,542430	99.70	99.67
4	-0,132954	-2,043790	0,134554	-8,723675	-0,348635	0,714420	-5,206013	0,294000	0,407092	99.53	99.46
5	-1,556998	-1,448930	0,444626	-7,152794	-0,009653	0,969220	-2,067454	1,624840	0,472360	99.74	99.71
6	-1,969208	0,111916	1,679230	-1,574085	0,313747	0,300664	-3,658625	-0,095452	0,432229	98.79	98.64
7	-3,164188	-0,672280	1,533210	-6,680782	0,012294	0,575260	-1,758831	1,259300	0,959420	99.53	99.49
8	-0,419151	-1,235290	0,273077	-6,002666	0,011500	0,950600	-1,433122	1,531250	0,447664	99.79	99.77
9	-5,083204	-0,301056	1,572410	-2,767997	0,056889	0,404838	-1,451276	1,279390	0,394891	99.05	98.96
10	-2,748775	-0,300909	0,724710	-2,184923	0,540960	0,762930	-0,923200	1,375920	0,412237	99.76	99.73
11	-1,679807	-1,014790	0,563010	-6,052857	0,012235	0,519890	-1,068968	0,937370	0,376614	99.94	99.94
12	-1,188573	-1,776740	0,448742	-7,988960	0,008903	1,090250	-1,427782	1,872780	0,466039	99.88	99.86
13	-0,574210	-2,903250	0,663460	-4,530032	-0,062230	2,360330	-0,848340	2,820440	0,635530	99.75	99.74
14	-1,293227	-1,143660	0,535570	-3,139626	-0,016136	0,981470	-1,178962	1,080450	0,518420	98.87	98.74
15	-1,477974	-1,656200	0,539490	-6,396721	-0,004048	0,911890	-1,324196	1,682660	0,517440	99.92	99.91
16	-0,991225	-1,335740	0,350056	-5,979172	0,007796	0,833000	-1,544183	1,353380	0,412923	99.80	99.77
17	-0,878455	-1,368570	0,359219	-5,209216	0,011172	0,787920	-1,207795	1,320060	0,404544	99.84	99.83
18	-1,618936	-0,914340	0,469273	-3,705613	0,018238	0,818300	-1,932899	1,054480	0,480837	99.89	99.88
19	1,980955	2,202550	0,333445	-2,063183	-0,546350	0,835940	-2,911095	0,705110	1,334760	98.39	98.20

Table 3: *Regression models for the geometry and the quality characteristics for stainless steel.*

Coeff.	Regression model	R^2 %	$R^2_{(adj)}$%
a_1	$-0.51070332+2.9476709x_3-0.78436911x_2x_2-2.6501947x_3x_3-1.0937238x_5x_5-2.2737272x_1x_3+0.26842274x_1x_4$	0.87361	0.81042
b_1	$-1.4233477+0.15946073x_1-0.2726584x_2+1.411227x_3+0.46498872x_4-0.30330783x_5-0.31695135x_2x_2+1.0031487x_3x_3-1.4008267x_1x_3+0.33852021x_2x_4+0.19601225x_3x_4$	0.97433	0.94225
c_1	$0.2457013-0.41353588x_3+0.01740861x_4-0.07081043x_5+0.29929228x_2x_2+1.1319594x_3x_3+0.24373887x_5x_5+0.03387758x_1x_2+0.24843x_3x_4+0.64236588x_1x_3-0.11390333x_1x_4$	0.97779	0.95002
a_2	-6.516416+0.81115202x1+0.30801097x2+0.80210999x3+1.2487342x4+2.6566892x3x3 +0.33065165x5x5+1.2221946x1x2-0.29594821x2x4+1.1309061x3x4+1.3779842x4x5-1.6275967x1x3-0.43927237x1x4	0.98353	0.9506
b_2	$-0.0738153+0.05431196x_1-0.04528773x_2-0.36832529x_3+0.1207588x_4+0.23421215x_3x_3+0.16413652x_5x_5+0.30037332x_1x_3+0.07087845x_4x_5-0.04372228x_1x_4$	0.85984	0.71967
c_2	$0.92701875+0.22492582x_1+0.28662958x_3-0.22144542x_4-0.57669733x_3x_3-0.30078285x_2x_4-0.158172x_3x_4+0.36450524x_1x_2-0.35959058x_1x_3$	0.79901	0.63822
a_3	$0.75093662x_1-0.75582384x_3+1.7820196x_4-4.9654962x_5+0.7030131x_2x_2-1.8286774x_4x_4-0.2008433x_2x_4-0.60696766x_3x_4-2.6697512x_4x_5-1.478161x_1x_4+1.4753859x_1x_5$	0.96279	0.91628
b_3	$1.2918862+0.08382981x_1+0.2388771x_2-0.38913532x_3-0.3368409x_5+0.69258346x_2x_2-0.37168074x_4x_4+0.94198611x_5x_5-0.52021755x_1x_4-0.24646391x_2x_4-0.3628205x_3x_4$	0.95656	0.90227
c_3	$0.42589758-0.03601233x_1+0.07368366x_2+0.4278724x_3-0.03391621x_4+0.13997065x_2x_2+0.19641134x_3x_3-0.05249007x_4x_4-0.13613425x_3x_4-0.28174215x1x_3-0.05804056x_1x_4+0.10927779x_1x_5$	0.98727	0.96728

In order to make prediction of the shapes of the welds in the whole experimental region of the process parameters (Table 1), not only in the experimental points, regression models are estimated for the coefficients a_1, b_1, c_1, a_2, b_2, c_2, a_3, b_3, c_3, depending on the coded values of the process parameters $\vec{p}$: $a_1(\vec{p})$, $b_1(\vec{p})$, $c_1(\vec{p})$, $a_2(\vec{p})$, $b_2(\vec{p})$, $c_2(\vec{p})$, $a_3(\vec{p})$, $b_3(\vec{p})$, $c_3(\vec{p})$.

The data processing is carried out in a coded scale, in order to avoid problems related to a possible multicollinearity or other numerical problems in the evaluation of the coefficients of regression and bad prediction values of the indicator of the quality.

The estimated regression models are presented in Table 3 for the EBW process parameter names p_1- p_5 in Table 1 and coded in a range from -1 to 1 values. Conversion from natural (Z_i) into coded (x_i) values can be done according to the formula:

$$p_i = \frac{2Z_i - \left(Z_{\min,i} + Z_{\max,i}\right)}{Z_{\max,i} - Z_{\min,i}}. \qquad (6)$$

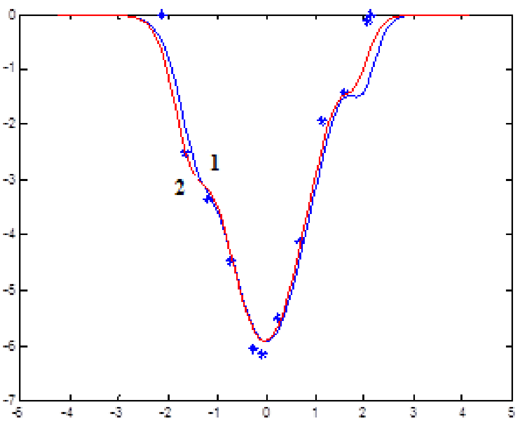

Fig. 3 *Weld cross-section: weld width B=4.24 mm, weld depth H = 6.16 mm at process parameters: L= 6 mm, F = 10 kHz, γ = 0, v = 5 mm/s, I_b = 45 mA,*
('' – experimental data, 1 – individual Gaussian functions, 2 – general Gaussian functions)*

In Table 3 are presented also the determination coefficients R^2 and adjusted determination coefficients R_{adj}^2 – the square of the multiple correlation coefficients. It can be seen that the models are good enough to be used for prediction of the weld shapes. The regression models for the coefficients in the general Gaussian function (1) are obtained from coefficients individual from Gaussian models (4) for the prediction of the shapes of the welds in the whole experimental region of the process parameters.

In Fig. 3 and Fig. 4 are presented for verification experimental data, individual Gaussian function and general Gaussian function for two experimental cases:

case 1: process parameters: L= 6 mm, F = 10 kHz, γ = 0, v = 5 mm/s, Ib = 45 mA; obtained geometry parameters: weld width B=4.24 mm, weld depth H = 6.16 mm;

case 2: process parameters: L= 6 mm, F = 10 kHz, γ = 0, v = 5 mm/s, I_b = 64.5 mA; weld width B=5.26 mm, obtained geometry parameters: weld depth H = 8.29 mm.

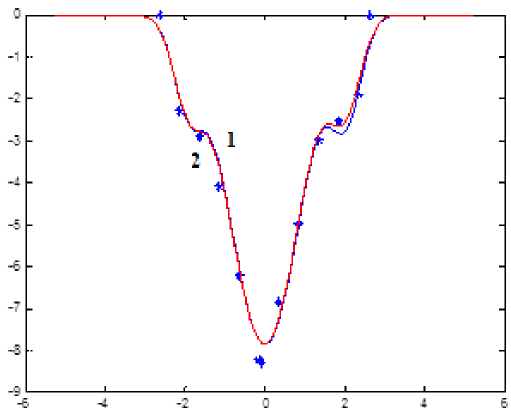

Fig. 4 *Weld cross-section: weld width B=5.26 mm, weld depth H = 8.29 mm at process parameters: L= 6 mm, F = 10 kHz, γ = 0, v = 5 mm/s, I_b = 64.5 mA*
('' – experimental data, 1 – individual Gaussian functions, 2 – general Gaussian functions)*

4. Conclusions

In this article it is demonstrated, that on base of statistical analysis of the experimental and or calculated data is possible to predict technological results as well as to make a choice of the processing parameters for obtaining desirable shapes and dimensions at joining of metal parts by electron beam welding.

The reported statistical model methodology is able to estimate relations that are difficult to be drawn by implementation of analytical thermal models and weld image observation. The models are applicable in computer expert system that can be built for operator advice at choice of welding regimes to meet customer's requirements and technical standards. These systems can be used at education and training of the personal and at prognostication and optimization of EB welding technology.

In order to improve the estimated models it is possible to perform more experimental runs, in order to estimate also the repeatability of the result. Another way to increase the accuracy of the models is to look for extending of the tests with parameters that not taken into account at previous experimental series, for example distance gun-sample surface, focus position, etc.

Acknowledgements

The work has been supported by the Bulgarian National Scientific Fund under contract DN17/9.

References

[1]. Koleva E., G. Mladenov, Experience on electron beam welding, Chapter 4 in book "Practical Aspects and Applications of Electron Beam Irradiation", Editors Team: M. Nemtanu, M. Brasoveanu, Transword Research Network, Trivandrum, India, pp. 95-133, 2011

[2]. Ольшанская Т.В., Федосеева Е.М., Колева Е.Г. Построение тепловых моделей при электронно-лучевой сварке методом функций Грина. Вестникпермского Национального Исследовательского Политехнического Университета, Машиностроение, Материаловедение, 2017 (3).

[3]. Yanhong Tian, Chunqing Wang, Danyang Zhu, Y. Zhou. Finite element modeling of electron beam welding of a large complex Al alloy structure by parallel computations. Journal of materials processing technology 199 (2008) 41–48.

[4]. Vuchkov I. N., Boyadjieva L. N., Quality improvement with design of experiments, The Netherlands, Kluwer Academic Publishers, 2001.

[5]. Koleva E., I. Vuchkov, Model-based approach for quality improvement of EBW applications in mass production, Vacuum 77, (2005), 423-428.